Journal Pre-proofs

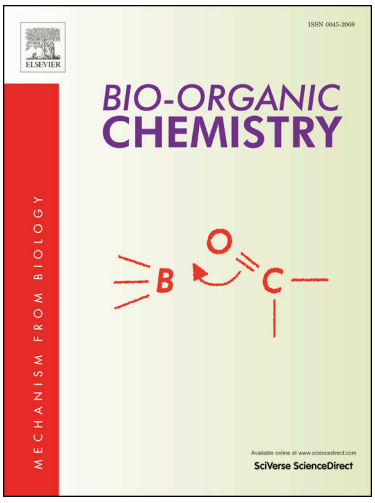

New nitroindazole-porphyrin conjugates: synthesis, characterization and anti-bacterial properties

Mohammed Eddahmi, Vera Sousa, Nuno M.M. Moura, Cristina J. Dias, Latifa Bouissane, Maria A.F. Faustino, José A.S. Cavaleiro, Ana T.P.C. Gomes, Adelaide Almeida, Maria G.P.M.S. Neves, El Mostapha Rakib

PII: S0045-2068(20)31291-8
DOI: https://doi.org/10.1016/j.bioorg.2020.103994
Reference: YBIOO 103994

To appear in: *Bioorganic Chemistry*

Received Date: 4 February 2020
Revised Date: 4 May 2020
Accepted Date: 2 June 2020

Please cite this article as: M. Eddahmi, V. Sousa, N.M.M. Moura, C.J. Dias, L. Bouissane, M.A.F. Faustino, J.A.S. Cavaleiro, A.T.P. Gomes, A. Almeida, M.G.P. Neves, E. Mostapha Rakib, New nitroindazole-porphyrin conjugates: synthesis, characterization and antibacterial properties, *Bioorganic Chemistry* (2020), doi: https://doi.org/10.1016/j.bioorg.2020.103994

New nitroindazole-porphyrin conjugates: synthesis, characterization and antibacterial properties

Mohammed Eddahmi,[a.b] Vera Sousa,[c] Nuno M. M. Moura,[a,*] Cristina J. Dias,[a] Latifa Bouissane,[b] Maria A. F. Faustino,[a,*] José A. S. Cavaleiro,[a] Ana T. P. C. Gomes,[b,*] Adelaide Almeida,[c] Maria G. P. M. S. Neves,[a] El Mostapha Rakib[b,*]

[a] *LAQV-REQUIMTE, Chemistry Department, University of Aveiro, 3810-193 Aveiro, Portugal.*
[b] *Laboratory of Organic and Analytic Chemistry, Faculty of Sciences and Technics, Sultan Moulay Slimane University, BP 523, 2300 Beni-Mellal, Morocco.*
[c] *CESAM and Biology Department, University of Aveiro, 3810-193 Aveiro, Portugal.*

Abstract

The synthesis of new porphyrin-indazole hybrids by a Knoevenagel condensation of 2-formyl-5,10,15,20-tetraphenylporphyrin and *N*-methyl-nitroindazole derivatives is reported. The target compounds were isolated in moderate to good yields (32-57%) and some of the isolated porphyrin-indazole conjugates showed good performance in the generation of singlet oxygen when irradiated with visible light. Their efficiency as photosensitizers in the photoinactivation of methicillin resistant *Staphylococcus aureus*–MRSA was evaluated. All derivatives showed to be able to photoinactivate the MRSA bacteria. Compound **3a** appears to be the most promising photosensitiser (PS) in the photoinactivation of these bacteria, despite being the least efficient in singlet oxygen generation. The addition of potassium iodide significantly potentiated the antimicrobial Photodynamic Therapy (aPDT) process mediated by all the analysed porphyrin-indazole conjugates. The combined action of nitroindazole-porphyrins with potassium iodide (KI) action appears to be promising in the photoinactivation of MRSA.

Keywords Tetrapyrrolic macrocycles; Porphyrin; Knoevenagel condensation; Indazole; Photosensitizer; Antimicrobial Photodynamic Therapy (aPDT); MRSA; Potassium iodide

1. Introduction

Porphyrins and indazoles derivatives are *N*-heterocycles with recognized relevance under different contexts. Porphyrins are well-known by their role in vital processes like respiration, photosynthesis, electron transportation and storage of relevant molecules [1, 2]. Additionally, not only these natural macrocycles but also the synthetic analogues display photophysical and photochemical features particularly attractive to be used in a wide range of fields like supramolecular chemistry, catalysis, electronic materials, sensors and medicine [3]. A relevant application of porphyrins in medicine is related with their role as photosensitizers in Photodynamic

Therapy (PDT) of tumours and more recently in the photodynamic inactivation of microorganisms (aPDT) [4-9]. The principles behind both treatments are the same and require the excitation of the photosensitizer (PS) by light in the presence of molecular oxygen to produce reactive oxygen species (ROS), namely singlet oxygen ($^1O_2$) responsible for the destruction of the cancer cells or for the inactivation of microorganisms [10-13]. These treatments have attracted great attention as an emerging clinical tool and as alternatives to traditional chemotherapy or antibiotic therapy. Since the photodynamic process is a multitarget approach and occurs only in the irradiated region, the possibility of photoresistance development is unlikely [11, 14-16].

Indazole derivatives are being successfully explored in the design of molecules with adequate features to be used for instance as anti-tumoral, antimicrobial and anti-inflammatory drugs [17-20]. It is known that the functionalization of the porphyrin core with moieties with relevant biological features can afford other porphyrins with an improvement in the biological performance [15, 21]. Having this in mind, this work reports the synthesis of new indazole-porphyrin derivatives *via* Knoevenagel condensation and their efficiency in the photoinactivation of a Gram-positive bacterium. As far as we know, this is the first study focused on the evaluation of the photodynamic effect of such hybrids as PSs in aPDT. One of the strategies envisaged by our research group to develop efficient PSs for aPDT is based on this functionalization of the porphyrin core with diverse heterocycles [22-25]. Knowing that certain heterocycles are active against trypanosomes, in 2013 we reported the synthesis of β-substituted porphyrins linked, *via* an amine/imine bond, to aminotriazole, isoniazid and aminothiadiazoles and their potentiality to act as PSs against leishmaniasis was evaluated [22]. All the hybrids revealed to be $^1O_2$ generators and molecular modelling and docking calculations showed that all these PSs have higher values of relative affinity to the leishmanial arginase than current drugs, classifying them as prototypes for future cutaneous leishmaniasis agents. Under the same context of developing efficient PSs for aPDT new porphyrin/4-quinolone conjugates were successfully synthetized *via* a palladium-catalyzed amination [23]. These PSs were studied in the photoinactivation of *S. aureus* showing high bacterial inactivation rates (> 6.0 log). The Heck coupling was also selected to obtain another series of porphyrin/4-oxoquinoline conjugates with excellent photosensitizing action towards *S. aureus* [24]. More recently, new cationic porphyrin-imidazole derivatives were synthesised by Radziszewski reaction. These PSs were able to photoinactivate *E. coli* and it was also shown that their inactivation profile was improved in the presence of KI [25].

In this context, 2-formyl-5,10,15,20-tetraphenylporphyrin **1** has revealed to be a versatile template for the porphyrinic core modification [26]. In fact, β-formyl porphyrins can be easily manipulated by recurring to different approaches namely those based on McMurry, Schiff's base, Horner-Emmons, Grignard, Wittig, cycloaddition and Knoevenagel reactions [27].

Under the context of the Knoevenagel condensation, Ponomarev and co-workers reported the first condensations involving the Cu(II) complex of 2-formyl-porphyrin **1** with malonic acid and its methyl or ethyl esters and the corresponding porphyrin derivatives in yields higher than 87% have been obtained [28]. A decade later, Chen and co-workers explored this approach to couple a series of formyl derivatives bearing olefin bridges of varying lengths in the β-pyrrolic position of

the Ni(II) complex of *meso*-tetrakis(4-isopropylphenyl)porphyrin, with diethyl malonate, ethyl cyanoacetate, malononitrile, and *N*,*N'*-diethylthiobarbituric acid in the presence of aluminium oxide [29, 30].

More recently, Mandeep, Sankar and co-workers used the condensation of malonitrile or cyanoacetic acid with a series of β-formyl *meso*-tetraarylporphyrins as free-bases or coordinated with different metal ions (*e.g.* Ni(II), Cu(II)) to afford the expected products in excellent yields. In their studies it was evaluated the potentialities of this type of derivatives to be used as colorimetric chemosensors in the CN^- and F^- detections [31-33].

The Knoevenagel condensation between the Zn(II) complex of 2-formyl porphyrin derivatives and a series of adequate methylene active compounds is also being successfully explored by different researcher groups in the development of sensitizers for Dye-Sensitized Solar Cells (DSSC). Attractive power conversion efficiencies ranging from 5 to 8% have been reported [34-43].

In 2017, Officer *et al.* reported that the Knoevenagel condensation between 2-formyl porphyrin **1** and a series of *para* substituted phenylacetonitriles afforded the expected porphyrinylacetonitriles. The authors mentioned that the reactions with phenylacetonitriles bearing strong electron-donating groups need to be mediated with strong bases, such as 1,8-diazabicyclo[5.4.0]undec-7-ene (DBU) or KO*t*Bu. The authors explored this approach to prepare symmetrical and unsymmetrical porphyrin dyads by using 1,4-phenylenediacetonitrile, in the presence of DBU or sodium methoxide [44].

Recently, we reported an efficient synthetic access to a series of nitroindazolylacetonitriles from the reaction of adequate *N*-methyl-nitroindazole with 4-chlorophenoxyacetonitrile [45] (*vide* infra **Scheme 1**). Considering the potentialities of these compounds to act as active methylene components and the reactivity of 2-formylTPP (**1**) in Knoevenagel condensations, we envisaged that this approach could allow the access to porphyrinic derivatives decorated with nitroindazole units.

So, herein we report the synthetic access to new porphyrin-indazole hybrids **3a-e** by recurring to the Knoevenagel reaction between the *N*-methyl-nitroindazolylacetonitriles **2a-e** and the 2-formyl-5,10,15,20-tetraphenylporphyrin (**1**) (**Scheme 1**). The efficacy of these derivatives to generate singlet oxygen prompted us to evaluate also their photodynamic efficacy against a MRSA *Staphylococcus aureus* bacterium. *S. aureus* is a Gram-positive bacterium which in normal conditions is commensal in humans and animals, but can easily become pathogenic, causing frequently skin, respiratory, bone, soft tissue and endovascular infections [46]. As *S. aureus* often develops resistance to multiple antibiotics, namely to β-lactam antibiotics such as methicillin (MRSA strains) [47], this bacterium is one of the major causes of health care and community associated infections [48][49]. The aPDT experiments were also performed with combinations of PSs **3a-e** with potassium iodide (KI), a well-known potentiator of aPDT effect [50].

2. Results and Discussion

2.1. Synthesis and characterisation

The preparation of the porphyrin-nitroindazole hybrids **3a-e** is outlined in scheme 1 and as it was mentioned it involved the Knoevenagel condensation between the 2-formyl-5,10,15,20-tetraphenylporphyrin **1** and the appropriate *N*-methyl-nitroindazolylacetonitriles **2a-e.** These derivatives were obtained *via* vicarious nucleophilic substitution of the adequate *N*-methyl-nitroindazole with 4-chlorophenoxyacetonitrile accordingly with a synthetic approach recently described by our group [45]. The formyl component was obtained from 5,10,15,20-tetraphenylporphyrin through a well-established sequence involving copper complexation, Vilsmeier formylation, demetallation of the iminium salt, followed by basic hydrolysis [51, 52].

The reactions were performed in the presence of piperidine at refluxing tetrahydrofuran (THF) for 36 h when the thin layer chromatography (TLC) control showed the presence of a new compound as the main fraction. After the work-up and purification by silica gel column chromatography, the new derivatives were identified as the expected porphyrin-nitroindazole hybrids **3a-e.** The new conjugates were isolated in yields ranging from 32 to 57% and it was possible to recover 19% of the starting porphyrin **1**; attempts to favour the conversion by increasing the reaction time led to the decomposition of the desired products. Also, other attempts to improve the efficacy of these reactions by changing the base (*e.g.* potassium carbonate, potassium hydroxide, ammonium acetate or DBU) or alternatively by using other solvents (*e.g.* a mixture of THF/methanol (MeOH) (2:1) or toluene) gave rise to a worse performance like the recovery of the starting porphyrin or the isolation of the desired products in lower yields (*e.g.* 20% with DBU).

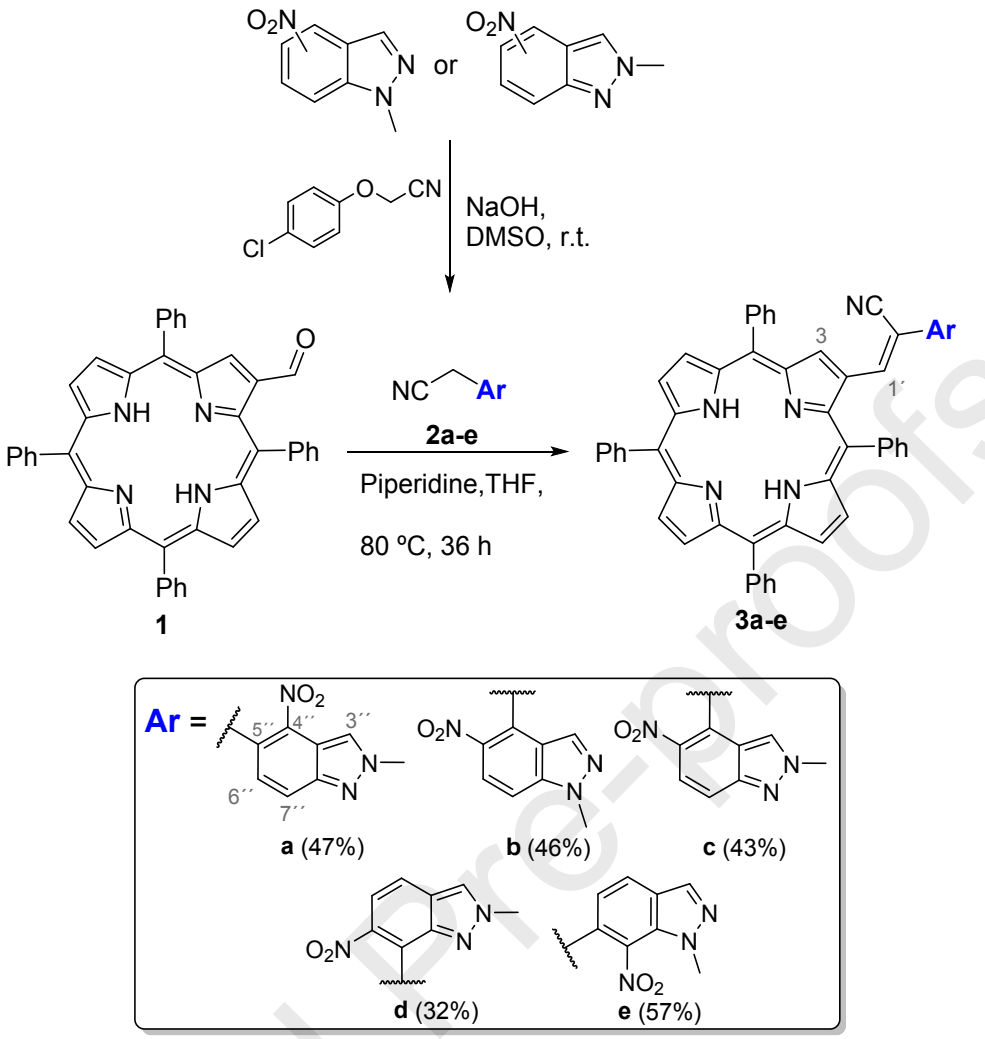

Scheme 1: β-functionalization of 2-formyl-5,10,15,20-tetraphenylporphyrin with *N*-methyl-nitroindazoles via Knoevenagel condensation.

The structure of each new porphyrin-nitroindazole hybrid **3a-e** was established considering its mass spectrum, which shows the $[M+H]^+$ ion peak at *m/z* = 841.3, and from NMR studies (see ESI, Figures S1-S26). In the ^{1}H NMR spectrum of each derivative **3a-e**, the expected singlet due to the resonance of the β-pyrrolic proton at H-3 appears at ca. *δ* 9.7 ppm. The remaining six β-pyrrolic protons generates signals centred at *ca. δ* 9.0 and *δ* 8.7 ppm. A remarkable signal that proves the success of the Knoevenagel condensation in each case is a singlet with a chemical shift ranging from *δ* 6.80 to *δ* 7.02 ppm which is due to the resonance of the vinylic proton.

The resonances of the protons from each nitroindazole moiety generate three signals in the aromatic region, two doublets ranging from *δ* 8.30 to 7.01 ppm due to the resonance of the two protons from the six-membered ring and a singlet between *δ* 8.04 and *δ* 8.57 ppm due to the resonance of the proton from the pyrazolic ring. In the ^{1}H NMR spectra of compounds **3d** and **3e** such signal appears embedded in a multiplet which includes the resonances of the *ortho* protons from the *meso* phenyl rings. The resonance of the *N*-methyl protons of **3d** and **3e** appears in the aliphatic region as a singlet centred respectively at *δ* 4.17 and *δ* 4.37 ppm. The singlet at *δ*

-2.6 ppm is in accordance with the free-base form of the porphyrin-nitroindazole derivative and it is due to the resonances of the inner core *N*-H protons.

2.2. Photophysical properties

The photophysical characterization of compounds **3a-e** was performed in DMF solution at 298 K. **Figure 1** shows the absorption, emission and excitation spectra of compound **3c** as a representative example of the porphyrin-imidazole derivatives' series.

The absorption spectrum shows the typical features of free base porphyrins due to π–π* transitions with the highly intense Soret band due to the $S_0 \rightarrow S_2$ allowed transition at *ca.* 430 nm and four weak Q bands due to the transition from $S_0 \rightarrow S_1$ between 523 and 658 nm [53]. The introduction of the indazole moiety at the β-pyrrolic position of the porphyrinic macrocycle induces a significant red-shift in the Soret band (*ca.* 15 nm) and in the Q bands (*ca.* 10 nm) in all the porphyrin-indazole derivatives UV-Vis spectra relatively to the reference TPP. The perfect resemblance between the absorption and the excitation spectra rules out the presence of any emissive impurity.

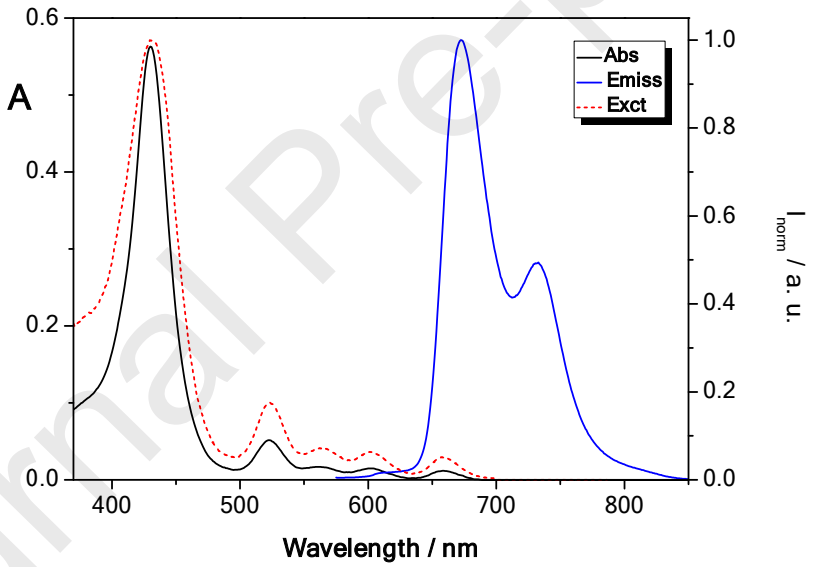

Figure 1: Absorption (Abs) and normalized emission (Emiss) and excitation (Exct) spectra of compound **3c** in DMF at 298 K ([**3c**] = 5.00 x 10^{-6} M, λ_{exc3c} = 523 nm and $\lambda_{emiss3c}$ = 731 nm).

The steady-state fluorescence emission spectra of the porphyrin-indazole derivatives **3a-e** were performed in DMF after their excitation at *ca.* 520 nm (see Figure 1 and Figure S27 in the SI). The emission spectra of all the new derivatives present the typical features of *meso*-tetraarylporphyrins, two bands centred in the range between 671-676 nm and at *ca.* 730 nm, where the first vibrational mode of the fluorescence is much more pronounced than the second one. The emission bands can be assigned to Q_x(0-0) and Q_x(0-1) transitions, typical of free base porphyrins with a D_2h symmetry due to a nearly unchanged vibronic state upon excitation [54,

55]. The porphyrin-indazole derivatives show low Stokes shifts (12-18 nm), indicating that the spectroscopic energies are similar to the relaxed energies of the lowest singlet excited state S1, suggesting the occurrence of a minor geometric relaxation in the first excited state.

The fluorescence quantum yields (Φ_{Flu}) of the studied compounds **3a-e** were determined by the internal reference method with respect to a solution of TPP as standard (Φ_{Flu} = 0.11) [56-58] and show values slightly lower than those due to the reference, ranging from 0.07 to 0.09, indicating the quenching of the porphyrin excited singlet state by the unit linked at the *beta* position; probably that can be attributed to an alteration of the planarity of the porphyrinic core due to the presence of the indazole moiety that can be responsible for a more reduced π-electron mobility.

2.3. Singlet oxygen generation

In order to evaluate the potentialities of the new derivatives to be used as photosensitizers in antimicrobial photodynamic therapy, it was determined their ability to generate $^1O_2$. This efficacy was estimated using *9*,10-dimethylanthracene (DMA) as a scavenger of the $^1O_2$ produced by the combined action of light, dissolved oxygen and porphyrin. DMA reacts selectively with the $^1O_2$ generated through a [4+2] cycloaddition reaction affording a non-fluorescent 9,10-endoperoxide species [59]. As reference, it was used 5,10,15,20-tetraphenylporphyrin (**TPP**) which has been reported as a good oxygen generator [60].

The results obtained for the capability of porphyrin-indazole derivatives **3a-e** to generate $^1O_2$ are presented in Table S1 and in general all the studied compounds are able to produce singlet oxygen. However, compound **3a** is the less efficient one to produce this cytotoxic species when compared with **TPP** (Φ_Δ = 0.10 *vs* Φ_Δ = 0.65) and with the other porphyrin-indazole derivatives **3b-e**. Compounds **3b**, **3d** and **3e** showed to be the best singlet oxygen generators with singlet oxygen quantum yields ranging from Φ_Δ =0.45 to Φ_Δ = 0.53 (efficiency ≈ 70 to ≈ 80 % in relation to the one from the reference **TPP)** (Table S1, SI). Compound **3c** (Φ_Δ = 0.32) presents a moderate ability to generate $^1O_2$, inducing a ≈ 50 % lower DMA photooxidation than that caused by **TPP**. No photooxidation of DMA was observed in the absence of a photosensitizer.

The ability of the porphyrin-indazole derivatives to generate $^1O_2$ after being exposed to light and oxygen makes them potential candidates to be used as photosensitizers in the photodynamic inactivation of microorganisms.

2.4. Detection of iodine formation in the presence of porphyrin-indazole hybrids 3a-e.

In order to verify if the efficacy of each porphyrin-indazole hybrids **3a-e** as PSs could be potentiated by the presence of potassium iodide, a simple assay to detect the formation of molecular iodine in their presence was performed. The inorganic salt in the presence of $^1O_2$ can afford peroxyiodide ($HOOI_2^-$) which can give rise to the bactericidal species molecular iodine (I_2/I_3^-

), hydrogen peroxide and iodine radicals ($I_2^{\cdot-}$) (*vide infra*). So, the detection of iodine formation can allow us to elucidate, before the biological assays, if the photodynamic efficiency of each PS can be improved by the presence of KI and if it is related with the antimicrobial iodine formation [50]. In this sense, each compound at a concentration of 5.0 μM was irradiated with white light in the absence and in the presence of KI at a concentration of 100 mM for pre-defined irradiation times and the absorbance at 340 nm was monitored.

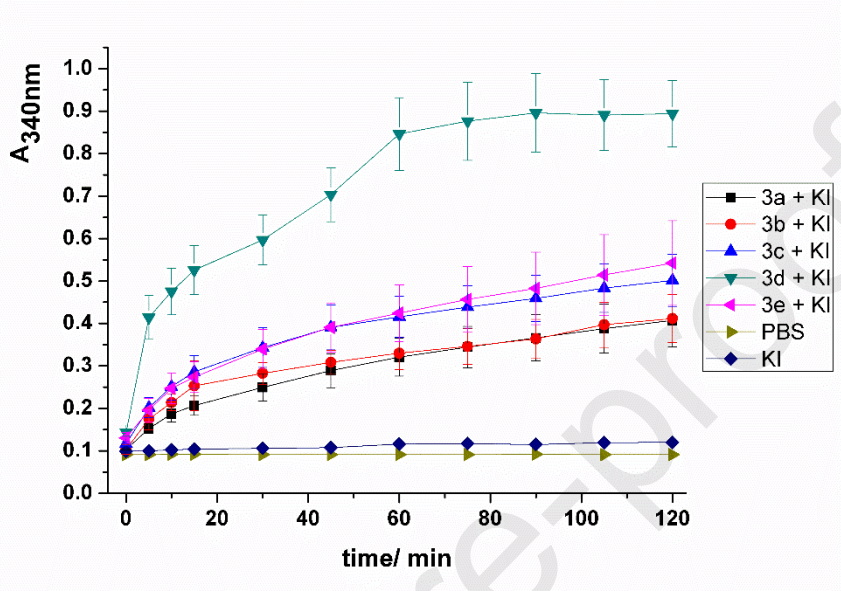

Figure 2: Monitoring the generation of molecular iodine, at 340 nm, after different irradiation times in the presence of each hybrid **3a-e** at 5.0 μM in the absence and in the presence of KI at 100 mM.

The results presented in Figure 2 show that the absorbance at 340 nm remained stable during the 120 min of irradiation when KI was irradiated in the absence of any one of the new adducts; the same profile was observed when the hybrids were irradiated in the absence of KI (data not shown). However, a different behaviour was observed when the PSs were irradiated in the presence of KI. Compound **3d** gave rise to the highest iodine production during the irradiation procedure. Compounds **3a**, **3b**, **3c** and **3e** also showed a gradual increase of the absorbance at 340 nm being compounds **3c** and **3e** slightly more effective in producing iodine than compounds **3a** and **3b**.

2.5. Photodynamic inactivation of MRSA using porphyrin-indazole derivatives 3a-e as PSs in the absence and in the presence of KI

The photodynamic efficacy of each porphyrin-indazole derivative **3a-e** against MRSA was evaluated at 5.0 μM in the absence and in the presence of 100 mM of KI (Figure 3). The KI concentration was chosen according with previous studies, which demonstrated that concentrations of this salt between 50 μM and 100 μM are capable to potentiate the photodynamic effect when combined with adequate PSs [25, 50, 61-63]. Moreover, it was also reported that higher concentrations than 100 μM can promote osmotic stress limiting the application of this approach in clinic area [50]. The aPDT experiments were carried out under white light irradiation

(380–700 nm) at an irradiance of 50 mW.cm^{-2} for 150 min. These irradiation conditions were optimized after several preliminary studies where we tested lower irradiance and shorter irradiation times (data not shown). The results summarized in Figure 3 show that the inactivation profile of MRSA with porphyrin derivatives **3a-e** is highly improved in the KI presence. In all cases, light, light plus KI and dark controls did not promote a decrease in the MRSA viability, showing that this bacterium is not affected in the absence of the PSs by irradiation or KI or in the absence of light by the PSs.

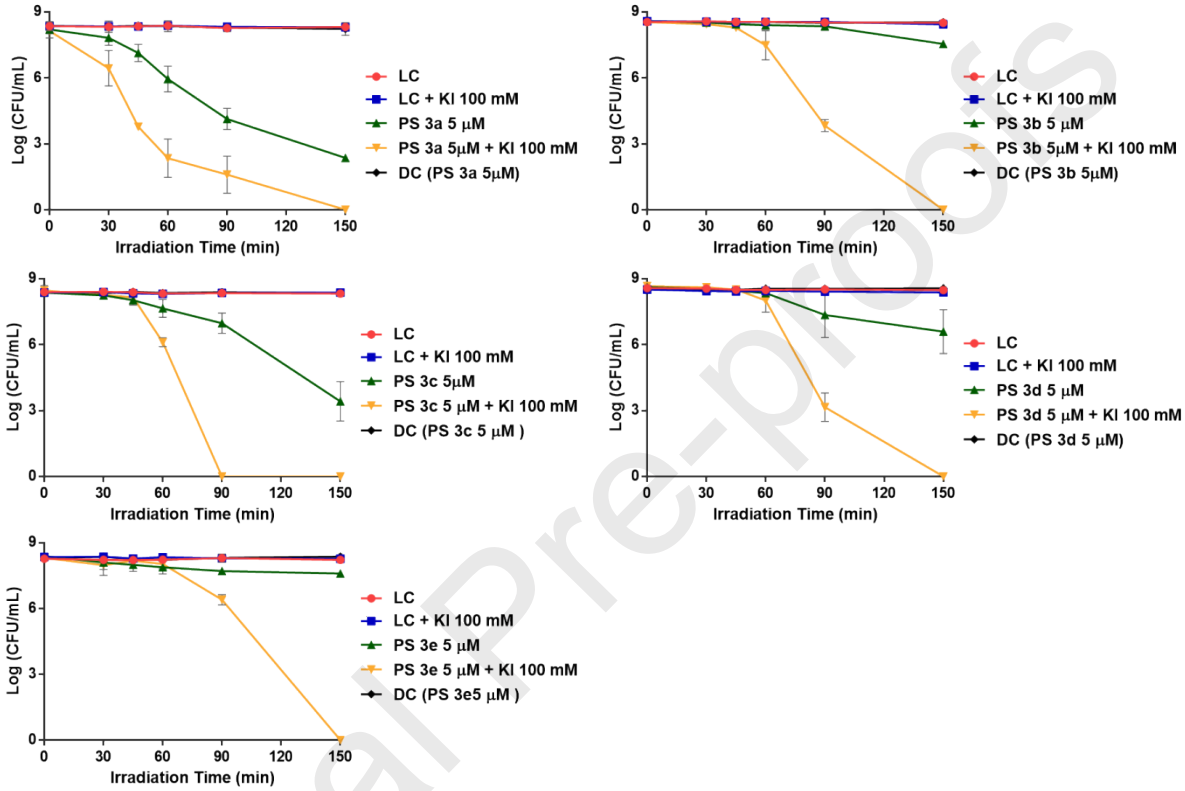

Figure 3: Photodynamic inactivation of MRSA in the presence of **3a** (A), **3b** (B), **3c** (C), **3d** (D) and **3e** (E) at 5.0 μM in PBS, without and with KI at 100 mM. The irradiations were performed with white light (380-700 nm) at 50 mW/cm^2. Values represent the average of three independent experiments with two replicates each; error bars indicate the standard deviation. Lines just combine the experimental points.

The results showed that the neutral porphyrins **3a** and **3c** are the most efficient photosensitizers when acting in the absence of KI (Figure 3A and 3C). These two PSs were capable to promote a decrease of 5.9 $\log_{10}$ (for **3a**) and 4.9 $\log_{10}$ (for **3c**) in the MRSA concentration after 150 min of aPDT treatment (ANOVA, $p < 0.05$). On the contrary, porphyrin-indazole derivatives **3b** and **3e** revealed to be the less efficient PSs (Figure 3B and 3E) when acting alone, causing just a small decrease in the MRSA viability, 0.9 and 0.6 $\log_{10}$, respectively, even after 150 min of irradiation (ANOVA, $p < 0.05$). The conjugate **3d** (Figure 3 D) showed a slight better performance causing a decrease of 1.8 $\log_{10}$ in MRSA viability after 150 min of irradiation (ANOVA, $p < 0.05$).

Trying to correlate the photodynamic profile of MRSA inactivation of porphyrin-indazole derivatives **3a-e** with the $^1O_2$ production, it is possible to observed that the PSs with the highest singlet oxygen production capacity (**3b**, **3d** and **3e**), were surprisingly the least effective in the MRSA photoinactivation. This fact can be due probably to their poor ability to interact with the bacterial membrane. Knowing that proteins and lipids from the cytoplasmic membrane and bacterial cells wall are the main targets of aPDT, if the PS interaction and/or its binding to these extracellular structures is limited, the inactivation efficiency is highly affected [64].

As it was already mentioned, the assays performed with **3a-e** combined with KI led to a considerable enhancement in the photodynamic efficiency of each conjugate. In all cases, although at different irradiation times, the combination PS + KI had promoted a decrease in the MRSA survival till the detection limit of the method. It is remarkable the results attained with porphyrin-indazole **3c** combined with KI (Figure 3 C), since it had promoted a decrease of 8.3 $\log_{10}$ (ANOVA, $p < 0.05$) in the MRSA concentration after 90 min of irradiation. For the remaining PSs, the total inactivation of MRSA was achieved after 150 min of aPDT protocol [decreases of *c.a*. 8.3 $\log_{10}$ (ANOVA, $p < 0.05$) (Figure 3 A, B, D, E). Nevertheless, the nitroindazole-porphyrins derivatives **3a** and **3c**, even in the absence of KI, were more effective to photoinactivate S. *aureus* than the aminolevulinic acid (ALA) [65] and hematoporphyrin [66, 67], the only two PSs already approved to be used in aPDT.

Recent studies have shown that the addition of non-toxic salts such as KI to neutral and anionic PSs improve the photodynamic efficiency of a broad spectrum of PSs allowing a major decrease of the aPDT treatment time and the reduction of the PSs concentration [50]. All these studies suggested that the KI potentiation is caused by several parallel reactions which begins with the reaction of $^1O_2$ with KI producing peroxyiodide that can be decomposed into free iodine (I_2/I_3^-) and into reactive iodine radicals ($I_2^{\cdot-}$), along with peroxide species. Knowing this, it is possible to distinguish the entity responsible for the microbial killing by analysing the respective inactivation profile. An abrupt photoinactivation profile means that the principal contribution is due to the free iodine. However, if the curve shows a gradual profile, the short-lived reactive iodine species are the mainly killing species [50, 68].

The results achieved with the combination of the PSs **3a-e** with KI in the photoinactivation of MRSA showed the enormous potential of KI as a potentiator agent of the aPDT effect, improving the antimicrobial photodynamic activity of the less efficient compounds, such as **3b**, **3d** and **3e**. In what concerns the photoinactivation profile the results showed that the addition of KI to compound **3a** caused a gradual decrease of the MRSA concentration, however, in the case of combination of PSs **3b-3e** + KI an abrupt decrease in the bacterial survival is attained. These results seem to be in agreement with the study on the detection of molecular iodine formation (Figure 2), which indicates that combination of **3a** + KI has the lowest iodine production capability, which indicates the production of reactive iodine radicals ($I_2^{\cdot-}$) that justifies the gradual inactivation profile. The combination of PS **3d** + KI revealed to be the most efficient to produce free iodine (I_2/I_3^-) which can also justify the abrupt decrease in the MRSA concentration between 60 and 90 min of treatment [40].

3. Experimental section

3.1. General remarks

Melting points were measured using a Buchi Melting Point B-540 apparatus. Electrospray ionization mass spectra (ESI) were acquired with a Micromass Q-Tof 2 (Micromass, Manchester, UK), operating in the positive ion mode, equipped with a Z-spray source, an electrospray probe and a syringe pump. Source and desolvation temperatures were 80 ºC and 150 ºC, respectively. Capillary voltage was 3000 V. The spectra were acquired at a nominal resolution of 9000 and at cone voltages of 30 V. Nebulisation and collision gases were N_2 and Ar, respectively. Compound solutions in methanol were introduced at a 10 μL min^{-1} flow rate. ^1H and ^{13}C solution NMR spectra were recorded on Bruker Avance 500 (500 and 125 MHz, respectively) spectrometer. $CDCl_3$ was used as solvent and tetramethylsilane (TMS) as the internal reference; the chemical shifts are expressed in δ (ppm) and the coupling constants (*J*) in Hertz (Hz). Unequivocal ^1H assignments were made using 2D COSY ($^1H/^1H$), while ^{13}C assignments were made on the basis of 2D HSQC ($^1H/^{13}C$) and HMBC (delay for long-range *J* C/H couplings were optimized for 7 Hz) experiments. Elemental analyses were performed on a LECO CHNS-932 apparatus. Column chromatography was carried out using silica gel (Merck, 35-70 mesh). Analytical TLC was carried out on precoated sheets with silica gel (Merck 60, 0.2 mm thick).

All chemicals were used as supplied. Solvents were purified or dried according to the literature procedures [69]. The 2-formyl-5,10,15,20-tetraphenylporphyrin **1** was prepared from 5,10,15,20-tetraphenylporphyrinatocopper(II), *N,N*-dimethylformamide (DMF) and phosphorus oxychloride ($POCl_3$), according to literature procedure [52]. *N*-methyl-nitroindazoles **2a-e** were prepared by *N*-methylation of the appropriate nitro-1*H*-indazoles in the presence of NaOH, followed by reaction with 4-chlorophenoxyacetonitrile as reported in literature [45].

3.2. Synthesis

3.2.1. Knoevenagel reaction. General procedure: To a solution of 2-formyl-5,10,15,20-tetraphenylporphyrin **1** (20 mg, 31.2 mmol) in THF (5 mL) was added the appropriate *N*-methyl-nitroindazole **2a-e** (2 equiv., 62.4 mmol, 134.7 mg) and an excess of piperidine (0.5 mL). The mixture was stirred and heated under reflux for 36 h. After cooling, the solvent was removed under reduced pressure and the crude mixture was purified by column chromatography (silica gel) using toluene as the eluent. The isolated compounds were then crystallized from CH_2Cl_2-hexane and fully characterized by NMR, mass and UV-Vis techniques. The yields are summarized in Scheme 1.

(*Z*)-2-(2-(2-methyl-4-nitro-1*H*-indazol-5-yl)-acrylonitrile-3-yl-5,10,15,20-tetraphenylporphyrin, 3a.

^1H NMR (500 MHz, $CDCl_3$): *δ* 9.61 (1H, s, H-3), 8.98 (1H, d, *J* = 4.8 Hz, H-β), 8.90 (1H,d, *J* = 4.8 Hz, H- β), 8.82 (1H, d, *J* = 4.8 Hz, H-β), 8.79 and 8.78 (2H, AB system, *J* = 4.8 Hz, H-β), 8.72 (1H, d, *J* = 4.8 Hz, H-β), 8.57 (1H, s, H-3´´), 8.34-8.32 (2H, m, H-*o*-Ph), 8.23-8.19 (4H, m, H-*o*-

Ph), 8.15 (2H, d, *J* = 7.6 Hz, H-*o*-Ph), 8.01 (1H, d, *J* = 8.7 Hz, H-7´´), 7.87-7.73 (9H, m, H-*m,p*-Ph), 7.60 (2H, t, *J* = 7.6 Hz, H-*m*-Ph), 7.49 (1H, t, *J* = 7.6 Hz, H-*p*-Ph), 7.06 (1H, s, H-1´), 7.01 (1H, d, *J* = 8.7 Hz, H-6´´), 4.37 (3H, s, -CH_3), -2.61 (2H, s, *N*-H) ppm. **^{13}C NMR (125 MHz, $CDCl_3$)**: *δ* 149.6, 142.4, 142.2, 142.0, 141.7, 141.6, 138.7, 135.3, 134.63, 134.57, 134.4, 133.2-129.7 (C-β), 128.8, 128.21, 128.16, 127.91, 127.88, 127.85, 127.4, 127.0, 126.9, 126.8, 126.3, 124.4, 121.8, 120.6, 120.4, 119.3, 116. 9, 116.2, 109.5, 41.1 (-CH_3) ppm. **MS-ESI(+):** *m/z* 841.3 $[M+H]^+$. **HRMS-ESI**(+): *m/z* calculated to $C_{55}H_{37}N_8O_2$ $[M+H]^+$ 841.3034; found, 841.3061. **UV-Vis** (DMF): λ_{max} (log ε) 429 (4.70), 524 (3.59), 561 (3.20), 601 (3.07), 658 (3.09) nm.

(*Z*)-2-(2-(1-methyl-5-nitro-1*H*-indazol-4-yl)-acrylontrile-3-yl-5,10,15,20-tetraphenylporphyrin, 3b.

^{1}H NMR (500 MHz, $CDCl_3$): *δ* 9.68 (1H, s, H-3), 8.99 (1H, d, *J* = 4.8 Hz, H- β), 8.91 (1H,d, *J* = 4.8 Hz, H- β), 8.82 (1H, d, *J* = 4.8 Hz, H-β), 8.79-8.75 (3H, m, H-β), 8.36-8.34 (2H, m, H-*o*-Ph), 8.30 (1H, d, *J* = 9.3 Hz, H-6´´), 8.24-8.19 (4H, m, H-*o*-Ph), 8.08 (1H, s, H-3´´), 8.04 (2H, d, *J* = 7.4 Hz, H-*o*-Ph), 7.86-7.73 (9H, m, H-*m,p*-Ph), 7.52 (1H, d, *J* = 9.3 Hz, H-7´´), 7.34 (2H, t, *J* = 7.4 Hz, H-*m*-Ph), 7.15 (1H, t, *J* = 7.4 Hz, H-*p*-Ph), 6.84 (1H, s, H-1´), 4.19 (3H, s, -CH_3), -2.61 (2H, s, *N*-H) ppm. **^{13}C NMR (125 MHz, $CDCl_3$)**: *δ* 143.5, 141.9, 141.8, 141.72, 141.66, 140.8, 140.6, 135.3, 135.1, 134.63, 134.57, 134.2, 133.5-129.5 (C-β), 129.1, 128.2, 127.90, 127.86, 127.7, 127.2, 127.0, 126.9, 126.8, 126.4, 124.1, 123.2, 121.8, 120.6, 120.4, 119.5, 116.7, 109.7, 104.9, 36.2 (-CH_3) ppm. **MS-ESI(+):** *m/z* 841.3 $[M+H]^+$. **HRMS-ESI**(+): *m/z* calculated to $C_{55}H_{37}N_8O_2$ $[M+H]^+$ 841.3034; found, 841.3052. **UV-Vis** (DMF): λ_{max} (log ε) 430 (5.18), 523 (4.16), 560 (3.67), 602 (3.64), 658 (3.56) nm.

(*Z*)-2-(2-(2-methyl-5-nitro-1*H*-indazol-4-yl)-acrylonitrile-3-yl-5,10,15,20-tetraphenylporphyrin, 3c.

^{1}H NMR (500 MHz, $CDCl_3$): *δ* 9.66 (1H, s, H-3), 8.99 (1H, d, *J* = 4.8 Hz, H- β), 8.91 (1H,d, *J* = 4.8 Hz, H- β), 8.83 (1H, d, *J* = 4.8 Hz, H-β), 8.80-8.74 (3H, m, H-β), 8.35-8.34 (2H, m, H-*o*-Ph), 8.23-8.18 (4H, *m*, H-*o*-Ph), 8.13-8.11 (2H, m, H-3" and H-6´´), 8.02 (2H, d, *J* = 7.4 Hz, H-*o*-Ph), 7.86-7.73 (10H, m, H-*m,p*-Ph and H-7´´), 7.34 (2H, t, *J* = 7.4 Hz, H-*m*-Ph), 7.21 (1H, t, *J* = 7.4 Hz, H-*p*-Ph), 6.80 (1H, s, H-1´), 4.24 (3H, s, -CH_3), -2.62 (2H, s, *N*-H) ppm. **^{13}C NMR (125 MHz, $CDCl_3$):** *δ* 149.2, 144.0, 141.0, 141.72, 141.70, 141.68, 141.2, 135.3, 134.62, 134.56, 134.2-129.5 (C-β), 128.2, 127.93, 127.89, 127.8, 127.7, 127.2, 127.0, 126.9, 126.8, 126.1, 122.2, 122.0, 121.7, 120.6, 120.5, 119.5, 118.9, 116.8, 105.6, 41.2 ppm. **MS-ESI(+):** *m/z* 841.3 $[M+H]^+$. **HRMS-ESI**(+): *m/z* calculated to $C_{55}H_{37}N_8O_2$ $[M+H]^+$ 841.3034; found, 841.3057. **UV-Vis** (DMF): λ_{max} (log ε) 430 (5.03), 523 (4.02), 560 (3.56), 602 (3.52), 658 (3.42) nm.

(*Z*)-2-(2-(2-methyl-6-nitro-1*H*-indazol-4-yl)-acrylonitrile-3-yl-5,10,15,20-tetraphenylporphyrin, 3d.

^{1}H NMR (500 MHz, $CDCl_3$): *δ* 9.72 (1H, s, H-3), 8.97 (1H, d, *J* = 4.8 Hz, H- β), 8.89 (1H,d, *J* = 4.8 Hz, H- β), 8.81-8.75 (4H, m, H-β), 8.35-8.33 (2H, m, H-*o*-Ph), 8.24-8.19 (4H, m, H-*o*-Ph), 8.06-8.04 (3H, m, H-*o*-Ph and H-3´´), 7.84-7.72 (11H, m, H-*m,p*-Ph, H-4´´ and H-5´´), 7.30 (2H, t, *J* =

7.6 Hz, H-*m*-Ph), 7.12 (1H, t, *J* = 7.6 Hz, H-*p*-Ph), 7.02 (1H, s, H-1´), 4.22 (3H, s, -CH_3), -2.62 (2H, s, *N*-H) ppm. **^{13}C NMR (125 MHz, $CDCl_3$):** *δ* 146.5, 144.7, 144.6, 142.0, 141.8, 141.77, 141.75, 135.4, 134.62, 134.56, 134.3, 133.2-129.6 (C-β), 128.1, 127.9, 127.8, 127.5, 127.0, 126.84, 126.75, 124.8, 124.1, 121.9, 121.7, 121.6, 120.4, 120.3, 119.7, 117.4, 116.9, 116.9, 41.3 ppm. **MS-ESI(+):** *m/z* 841.3 $[M+H]^+$. **HRMS-ESI**(+): *m/z* calculated to $C_{55}H_{37}N_8O_2$ $[M+H]^+$ 841.3034; found 841.3040. **UV-Vis** (DMF): λ_{max} (log ε) 430 (5.24), 523 (4.34), 562 (3.83), 601 (3.79), 658 (3.73) nm.

(*Z*)-2-(2-(1-methyl-7-nitro-1*H*-indazol-4-yl)-acrylonitrile-3-yl-5,10,15,20-tetraphenylporphyrin, 3e.

^{1}H NMR (500 MHz, $CDCl_3$): *δ* 9.68 (1H, s, H-3), 8.99 (1H, d, *J* = 4.9 Hz, H-β), 8.91 (1H, d, *J* = 4.9 Hz, H-β), 8.82 (1H, d, *J* = 4.9 Hz, H-β), 8.79-8.74 (4H, m, H-β), 8.37-8.35 (2H, m, H-*o*-Ph), 8.29 (1H, d, *J* = 9.3 Hz, H-6´´), 8.23-8.18 (4H, m, H-*o*-Ph), 8.07-8.03 (3H, m, H-*o*-Ph and H-3´´), 7.84-7.72 (9H, m, H-*m,p*-Ph), 7.51 (1H, d, *J* = 9.3 Hz, H-5´´), 7.34 (2H, t, *J* = 7.7 Hz, H-*m*-Ph), 7.18-7.13 (1H, m, H-*p*-Ph), 6.84 (1H, s, H-1´), 4.17 (3H, s, -CH_3), -2.61 (2H, s, *N*-H) ppm. **^{13}C NMR (125 MHz, $CDCl_3$):** *δ* 143.5, 141.9, 141.8, 141.72, 141.67, 140.8, 140.6, 137.9, 135.3, 135.0, 134.64, 134.58, 134.2, 133.4-129.52 (C-β), 129.1, 128.3, 128.2, 127.91, 127.87, 127.7, 127.2, 127.0, 126.9, 126.8, 126.4, 125.3, 124.5, 124.1, 124.0, 123.2, 121.8, 120.6, 120.4, 119.5, 119.1, 116.7, 109.7, 104.9, 36.2 ppm. **MS-ESI(+):** *m/z* 841.3 $[M+H]^+$. **HRMS-ESI**(+): *m/z* calculated to $C_{55}H_{37}N_8O_2$ $[M+H]^+$ 841.3034; found 841.3048. **UV-Vis** (DMF): λ_{max} (log ε) 431 (5.33), 523 (4.16), 562 (3.82), 602 (3.80), 659 (3.74) nm.

3.3. Spectrophotometric and spectrofluorometric measurements

The absorption spectra were recorded on a UV-2501PC Shimadzu spectrophotometer and the fluorescence emission spectra were recorded on a Horiba Jobin-Yvon Fluoromax 3 spectrofluorimeter using DMF as solvent. The linearity of the fluorescence emission versus the concentration was checked in the concentration range used (10^{-4}-10^{-6} M). The correction of the absorbed light was performed when necessary. The studied solutions were prepared by appropriate dilution of the stock solutions up to 10^{-5}-10^{-6} M. All the measurements were performed at 298 K.

Fluorescence quantum yields of all porphyrin-nitroindazole derivatives **3a-e** were measured using a solution of 5,10,15,20-tetraphnylporphyrin (**TPP**) in dimethylformamide (DMF) as standard (Φ_{Flu} = 0.11) [58].

3.4. Singlet oxygen generation

Solutions of porphyrin-nitroindazole derivatives **3a-e** in DMF ($Abs_{430} \approx 0.50$) were aerobically irradiated in quartz cuvettes with monochromatic light (λ = 518 nm) in the presence of 9,10-dimethylanthracene (DMA, 30 μM). **TPP** was used as reference (Φ_Δ = 0.65) [70]. The kinetics of the photooxidation DMA in the presence of each PS was studied by following the decrease in its

absorbance at 378 nm and the result registered in a first-order plot. The kinetics of DMA photooxidation in the absence of any compound was also studied and no significant photodegradation of DMA was observed under the same irradiation conditions. The results are expressed as mean and standard deviation obtained from two independent experiments.

3.5. Detection of iodine formation

In a 96 wells microplate, appropriate volumes of each compound at 5.0 μM and also combinations of each compound at 5.0 μM and KI at 100 mM in PBS were incubated in the dark for 15 minutes and then irradiated with PAR white light at 25 W m^{-2}. The generation of iodine (I_2) was monitored by looking at the absorbance at 340 nm, at irradiation times 0, 5, 10, 15, 30, 45, 60, 75, 90, 105, and 120 min. Controls of phosphate buffered saline (PBS), pH 7.4 and KI were also performed.

3.6. Porphyrin-nitroindazole derivatives 3a-e stock solutions for antimicrobial photodynamic assays

Stock solutions of porphyrin-nitroindazole derivatives were prepared at 500 μM in dimethyl sulfoxide (DMSO) and stored in the dark. These solutions were sonicated for 15 minutes at ambient temperature before each experiment. For biological assays, the PS stock solutions were diluted to the final concentrations in PBS, pH 7.4.

3. 7. KI solution

Potassium iodide was provided by Biochem Chemopharma and the solutions of KI were prepared at 5M in sterile PBS, pH 7.4, and tested at 100 mM in photodynamic assays. These solutions were prepared immediately before each assay.

3.8. Light sources

The photodynamic effect of the porphyrin-nitroindazole derivatives **3a-e** was evaluated by exposing the bacterial suspension in the presence of each PS to white light (400-750 nm) delivered by a LED system (ELMARK – VEGA20, 20 W, 1400 lm) with fluence rate of 50 $mW.cm^{-2}$. All the irradiances were measured with a Power Meter Coherent FieldMaxII-Top combined with a Coherent PowerSens PS19Q energy sensor.

3.9. Bacterial strains and growth conditions

In this study was used a Gram-positive bacterium, *Staphylococcus aureus* DSM 25693, a methicillin-resistant (MRSA) strain that produces the staphylococcal enterotoxins S, E, A, C, H, G, and I. This Gram-positive bacterium was isolated from a biological low respiratory tract sample of hospitalized individuals [71].

The bacterium was maintained on Tryptic Soy Agar (TSA, Liofilchem) at 4 °C. Before each assay, a colony was transferred to 30 mL of Tryptic Soy Broth (TSB, Liofilchem) and incubated

for 18-24 h at 37 °C with constant stirring (120 rpm). Then 300 µL aliquots were transferred to new 30 mL TSB and incubated at the previous growth conditions, in order to reach the stationary phase, corresponding to a concentration of 10^8-10^9 colony forming units per mL (CFU.mL^{-1}).

3.10. Antimicrobial Photodynamic Therapy (aPDT) assays

The bacterial culture was grown overnight and was tenfold diluted in PBS, pH 7.4, to a final concentration of ~10^8 CFU mL^{-1}. The bacterial suspension was equally distributed in a 12-weel plate. Afterwards, the appropriate volumes of each porphyrin-nitroindazole derivatives **3a-e** were added to achieve a final desired concentration of 5.0 µM (corresponding to 1% DMSO) and 100 mM of KI (total volume was 5 mL per well). The samples were protected from light with aluminium foil and remained in the dark for 1 h to promote the porphyrin binding to MRSA cells. Light and dark controls were also carried out simultaneously with the aPDT procedure: the light control (LC) comprised a bacterial suspension exposed to the same light protocol, and the dark control (DC) comprised a bacterial suspension incubated with each porphyrin at 5.0 µM protected from light. In order to evaluate the effect of KI, a control comprising bacterial suspension and KI at 100 mM (LC + 100 mM KI) irradiated under the same conditions was also performed. After the incubation period, the samples and the LC were exposed to white light at 50 mW.cm^{-2} under stirring (120 rpm). The DC was maintained in the dark during the irradiation procedure. Photoinactivation efficiency of each PS was evaluated by quantifying the number of colony forming units (CFU) per volume (CFU mL^{-1}). Aliquots of samples and each control were taken at time 0 min (after incubation time) and at different irradiation times (30, 45, 60, 90 and 150 min). Serial dilutions were made and finally pour-plated in TSA. The petri plates were incubated at 37 °C for 18–24 h.

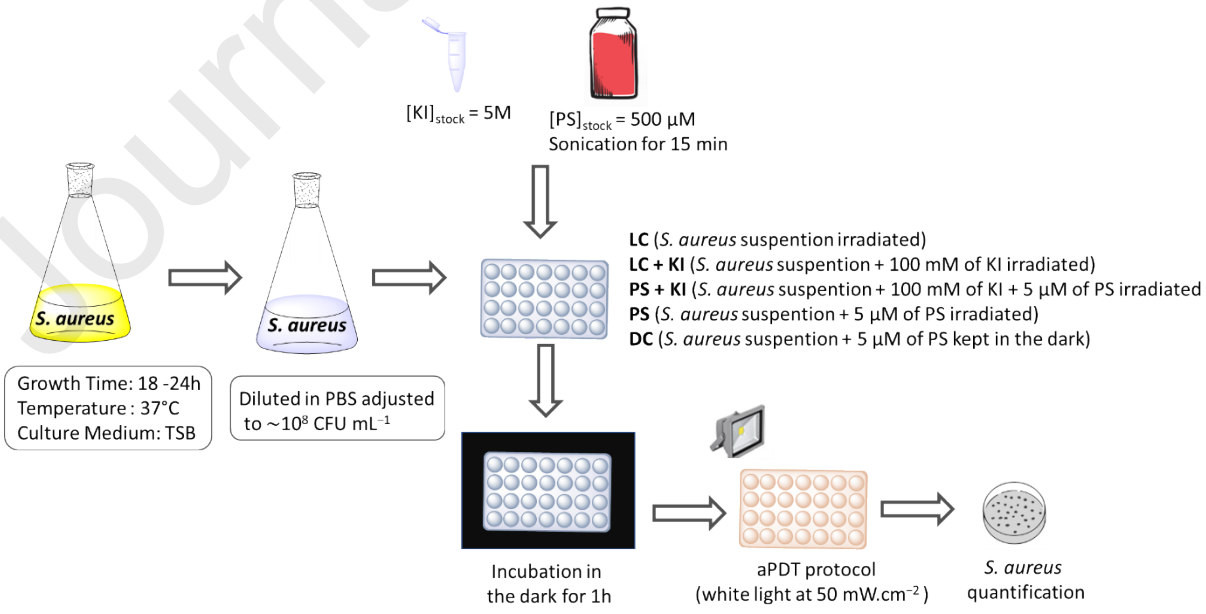

Figure 4: *Schematic representation of the photodynamic assays.*

3.11. Statistical

All experiments were performed in triplicate with two replicates per assay for each condition. The statistical analysis was performed with GraphPad Prism (GraphPad Software, San Diego, USA). Normal distributions were checked by the Kolmogorov–Smirnov test and the homogeneity of variance was verified with the Brown Forsythe test. ANOVA and Dunnet's multiple comparison tests were applied to assess the significance of the differences between the tested conditions. A value of $p < 0.05$ was considered significant.

4. Conclusions

The Knoevenagel condensation of 2-formyl-5,10,15,20-tetraphenylporphyrin with a series of *N*-methyl-nitroindazole derivatives showed to be an efficient synthetic approach to afford new porphyrin-indazole hybrids. The ability of these derivatives to generate oxygen singlet and molecular iodine when irradiated in the presence of KI are in accordance with the promising aPDT results obtained towards *S. aureus MRSA.* According to the American Society of Microbiology, compounds **3a** and **3c** in the absence of KI, are considered antimicrobials agents causing decreases in the bacterial concentration higher than 3 $\log_{10}$. The impact of these results are even higher when the photodynamic action was evaluated in the presence of KI, since all the hybrids were able to photoinactivate the MRSA bacteria until the detection limit of the method.

The impressive photoinactivation results of *S. aureus* obtained in this study with porphyrin-nitroindazole derivatives **3a-e** combined with KI, suggest that the use of these formulations to treat localized skin infections, caused by multiresistant strains such as MRSA, can be a promising alternative to antibiotics. Further *in vivo* studies with these compounds are needed in order to pave their potential to control *S. aureus* infections. Also, some experiments with *S. aureus* biofilms are necessary as this bacterium form frequently biofilms and the nitroindazoles could interfere with the quorum-sensing signaling and virulence factors.

Acknowledgements

The authors are grateful to the University of Aveiro and to the FCT/MCT for the financial support for the QOPNA research Unit (FCT UID/QUI/00062/2019), the LAQV-REQUIMTE (UIDB/50006/2020), CESAM (UUID/AMB/50017 - POCI-01-0145-FEDER-007638), and to the FCT project PREVINE (FCT-PTDC/ASPPES/29576/2017 through national funds (PIDDAC) and, where applicable, co-financed by FEDER, within the PT2020 Partnership Agreement, and to the Portuguese NMR Network. The authors also thank the Sultan Moulay Slimane University and the Transnational cooperation programs, FCT-CNRST (Morocco), for financial assistance (2019-2020). The research contract of N.M.M. Moura (REF.-048-88-ARH/2018) is funded by national funds (OE), through FCT – Fundação para a Ciência e a Tecnologia, I.P., in the scope of the framework contract foreseen in the numbers 4, 5 and 6 of the article 23, of the Decree-Law 57/2016, of August 29, changed by Law 57/2017, of July 19.

References

[1] W. Auwärter, D. Écija, F. Klappenberger, J.V. Barth, Porphyrins at interfaces, Nat Chem, 7 (2015) 105-20.

[2] K.M. Harmatys, M. Overchuk, G. Zheng, Rational Design of Photosynthesis-Inspired Nanomedicines, Acc Chem Res, 52 (2019) 1265-74.

[3] K.M. Kadish, Smith, K. M., Guilard, R., Handbook of Porphyrin Science, Singapore: World Scientific Publishing Company Co; 2010.

[4] S. Singh, A. Aggarwal, N.V.S.D.K. Bhupathiraju, G. Arianna, K. Tiwari, C.M. Drain, Glycosylated Porphyrins, Phthalocyanines, and Other Porphyrinoids for Diagnostics and Therapeutics, Chem Rev, 115 (2015) 10261-306.

[5] V. Almeida-Marrero, J.A. González-Delgado, T. Torres, Emerging Perspectives on Applications of Porphyrinoids for Photodynamic Therapy and Photoinactivation of Microorganisms, Macroheterocyles, 20 (2019) 22.

[6] M.Q. Mesquita, C.J. Dias, M.G.P.M.S. Neves, A. Almeida, M.A.F. Faustino, Revisiting Current Photoactive Materials for Antimicrobial Photodynamic Therapy, Molecules, 23 (2018) 47.

[7] M.A. Rajora, J.W.H. Lou, G. Zheng, Advancing porphyrin's biomedical utility via supramolecular chemistry, Chem Soc Rev, 46 (2017) 6433-69.

[8] S.R. De Annunzio, N.C.S. Costa, R.D. Mezzina, M.A.S. Graminha, C.R. Fontana, Chlorin, Phthalocyanine, and Porphyrin Types Derivatives in Phototreatment of Cutaneous Manifestations: A Review, Int J Mol Sci, 20 (2019) 3861.

[9] R. Yin, T. Agrawal, U. Khan, G.K. Gupta, V. Rai, Y.-Y. Huang, et al., Antimicrobial photodynamic inactivation in nanomedicine: small light strides against bad bugs, Nanomed, 10 (2015) 2379-404.

[10] P.R. Ogilby, Singlet oxygen: there is indeed something new under the sun, Chem Soc Rev, 39 (2010) 3181-209.

[11] X. Shi, C.Y. Zhang, J. Gao, Z. Wang, Recent advances in photodynamic therapy for cancer and infectious diseases, Wiley Interdiscip Rev Nanomed Nanobiotechnol, 11 (2019) e1560.

[12] Y.-Y. Wang, Y.-C. Liu, H. Sun, D.-S. Guo, Type I photodynamic therapy by organic–inorganic hybrid materials: From strategies to applications, Coord Chem Rev, 395 (2019) 46-62.

[13] L.K. McKenzie, H.E. Bryant, J.A. Weinstein, Transition metal complexes as photosensitisers in one- and two-photon photodynamic therapy, Coord Chem Rev, 379 (2019) 2-29.

[14] M.R. Hamblin, Antimicrobial photodynamic inactivation: a bright new technique to kill resistant microbes, Curr Opin Microbiol, 33 (2016) 67-73.

[15] H. Abrahamse, Michael R. Hamblin, New photosensitizers for photodynamic therapy, Biochem J, 473 (2016) 347-64.

[16] E. Alves, M.A.F. Faustino, M.G.P.M.S. Neves, A. Cunha, J. Tome, A. Almeida, An insight on bacterial cellular targets of photodynamic inactivation, Future Med Chem, 6 (2014) 141-64.

[17] R. Wiley, The Chemistry of Heterocyclic Compounds: Pyrazoles and Reduced and Condensed Pyrazoles, New York, NY,: John Wiley & Sons: 2009.; 2009.

[18] A.A. Hassan, A.A. Aly, H.N. Tawfeek, Indazoles: Synthesis and Bond-Forming Heterocyclization, in: E.F.V. Scriven, C.A. Ramsden (Eds.), Advances in Heterocyclic Chemistry, Vol 125, Elsevier Academic Press Inc, San Diego, 2018, pp. 235-300.

[19] I. Denya, S.F. Malan, J. Joubert, Indazole derivatives and their therapeutic applications: a patent review (2013-2017), Expert Opin Ther Pat, 28 (2018) 441-53.

[20] M. Eddahmi, N.M.M. Moura, L. Bouissane, M.A.F. Faustino, J.A.S. Cavaleiro, F.A.A. Paz, et al., Synthesis and Biological Evaluation of New Functionalized Nitroindazolylacetonitrile Derivatives, ChemistrySelect, 4 (2019) 14335-42.

[21] S. Shao, V. Rajendiran, J.F. Lovell, Metalloporphyrin nanoparticles: Coordinating diverse theranostic functions, Coord Chem Rev, 379 (2019) 99-120.

[22] V.R. Campos, A.T.P.C. Gomes, A.C. Cunha, M.G.P.M.S. Neves, V.F. Ferreira, J.A.S. Cavaleiro, Efficient access to β-vinylporphyrin derivatives via palladium cross coupling of β-bromoporphyrins with N-tosylhydrazones, Beilstein J Org Chem, 13 (2017) 195-202.

[23] P.N. Batalha, A.T.P.C. Gomes, L.S.M. Forezi, L. Costa, M.C.B.V. de Souza, F.d.C.S. Boechat, et al., Synthesis of new porphyrin/4-quinolone conjugates and evaluation of their efficiency in the photoinactivation of Staphylococcus aureus, RSC Adv, 5 (2015) 71228-39.

[24] F.S. Sagrillo, C. Dias, A.T.P.C. Gomes, M.A.F. Faustino, A. Almeida, A. Gonçalves de Souza, et al., Synthesis and photodynamic effects of new porphyrin/4-oxoquinoline derivatives in the inactivation of S. aureus, Photochem Photobiol Sci, 18 (2019) 1910-22.

[25] X. Moreira, P. Santos, M.A.F. Faustino, M.M.M. Raposo, S.P.G. Costa, N.M.M. Moura, et al., An insight into the synthesis of cationic porphyrin-imidazole derivatives and their photodynamic inactivation efficiency against Escherichia coli, Dyes Pigments, 178 (2020) 108330.

[26] J. A. S. Cavaleiro, A.C. Tomé, M. G. P. M. S. Neves, Handbook of Porphyrin Science, in: K.M.S. K. M. Kadish, R. Guilard (Ed.) Meso-tetraarylporphyrin derivatives: New synthetic methodologies, World Scientific Publishing Company Co., Singapore, 2010, pp. 193-294.

[27] A.F.R. Cerqueira, N.M.M. Moura, V.V. Serra, M.A.F. Faustino, A.C. Tomé, J.A.S. Cavaleiro, et al., β-Formyl- and β-Vinylporphyrins: Magic Building Blocks for Novel Porphyrin Derivatives, Molecules, 22 (2017) 1269.

[28] I.G. Rish, V.S. Pshezhetskii, K.A. Askarov, G.V. Ponomarev, Porphyrins. 20. Interaction of 2-formyl-5,10,15,20-tetraphenylporphyrin with ch acids, Chem Heterocycl Compd, 21 (1985) 777-81.

[29] C.-T. Chen, H.-C. Yeh, X. Zhang, J. Yu, Olefin-Mediated Interaction Observed for Nickel Tetraphenylporphyrins with an Acceptor Substituted on the β-Carbon, Org Lett, 1 (1999) 1767-70.

[30] H.-C. Yeh, C.-T. Chen, J. Yu, P.-C. Tsai, J.-K. Wang, Conformation and π-conjugation of olefin-bridged acceptor on the pyrrole β-carbon of nickel tetraphenylporphyrins: implicit evidence from linear and nonlinear optical properties, J Porphyrins Phthalocyanines, 11 (2007) 857-73.

[31] M.K. Chahal, M. Sankar, Porphyrin chemodosimeters: synthesis, electrochemical redox properties and selective ‘naked-eye’ detection of cyanide ions, RSC Adv, 5 (2015) 99028-36.

[32] K. Prakash, S. Manchanda, V. Sudhakar, N. Sharma, M. Sankar, K. Krishnamoorthy, Facile synthesis of β-functionalized “push-pull” Zn(II) porphyrins for DSSC applications, Dyes Pigments, 147 (2017) 56-66.

[33] M.K. Chahal, M. Sankar, Switching between porphyrin, porphodimethene and porphyrinogen using cyanide and fluoride ions mimicking volatile molecular memory and the ‘NOR’ logic gate, Dalton Trans, 45 (2016) 16404-12.

[34] Q. Wang, W.M. Campbell, E.E. Bonfantani, K.W. Jolley, D.L. Officer, P.J. Walsh, et al., Efficient Light Harvesting by Using Green Zn-Porphyrin-Sensitized Nanocrystalline TiO2 Films, J Phys Chem B, 109 (2005) 15397-409.

[35] W.M. Campbell, K.W. Jolley, P. Wagner, K. Wagner, P.J. Walsh, K.C. Gordon, et al., Highly Efficient Porphyrin Sensitizers for Dye-Sensitized Solar Cells, J Phys Chem C, 111 (2007) 11760-2.

[36] Z. Zeng, B. Zhang, C. Li, X. Peng, X. Liu, S. Meng, et al., A key point of porphyrin structure affect DSSCs performance based on porphyrin sensitizers, Dyes Pigments, 100 (2014) 278-85.

[37] G. Di Carlo, A.O. Biroli, F. Tessore, S. Caramori, M. Pizzotti, β-Substituted ZnII porphyrins as dyes for DSSC: A possible approach to photovoltaic windows, Coord Chem Rev, 358 (2018) 153-77.

[38] G. Di Carlo, A. Orbelli Biroli, M. Pizzotti, F. Tessore, V. Trifiletti, R. Ruffo, et al., Tetraaryl ZnII Porphyrinates Substituted at β-Pyrrolic Positions as Sensitizers in Dye-Sensitized Solar Cells: A Comparison with meso-Disubstituted Push–Pull ZnII Porphyrinates, Chem Eur J, 19 (2013) 10723-40.

[39] V.K. Narra, H. Ullah, V.K. Singh, L. Giribabu, S. Senthilarasu, S.Z. Karazhanov, et al., D–π–A system based on zinc porphyrin dyes for dye-sensitized solar cells: Combined experimental and DFT–TDDFT study, Polyhedron, 100 (2015) 313-20.

[40] G. Di Carlo, S. Caramori, V. Trifiletti, R. Giannuzzi, L. De Marco, M. Pizzotti, et al., Influence of Porphyrinic Structure on Electron Transfer Processes at the Electrolyte/Dye/TiO2 Interface in PSSCs: a Comparison between meso Push–Pull and β-Pyrrolic Architectures, ACS Appl Mater Interfaces, 6 (2014) 15841-52.

[41] T. Sakurada, Y. Arai, H. Segawa, Porphyrins with β-acetylene-bridged functional groups for efficient dye-sensitized solar cells, RSC Adv, 4 (2014) 13201-4.

[42] A. Covezzi, A. Orbelli Biroli, F. Tessore, A. Forni, D. Marinotto, P. Biagini, et al., 4D–π–1A type β-substituted ZnII-porphyrins: ideal green sensitizers for building-integrated photovoltaics, Chem Commun, 52 (2016) 12642-5.

[43] K. Sirithip, S. Morada, S. Namuangruk, T. Keawin, S. Jungsuttiwong, T. Sudyoadsuk, et al., Synthesis and characterization of β-pyrrolic functionalized porphyrins as sensitizers for dye-sensitized solar cells, Tetrahedron Lett, 54 (2013) 2435-9.

[44] R. Mitchell, K. Wagner, J.E. Barnsley, H. van der Salm, K.C. Gordon, D.L. Officer, et al., Synthesis and Light-Harvesting Potential of Cyanovinyl β-Substituted Porphyrins and Dyads, Eur J Org Chem, 2017 (2017) 5750-62.

[45] M. Eddahmi, N.M.M. Moura, L. Bouissane, A. Gamouh, M.A.F. Faustino, J.A.S. Cavaleiro, et al., New nitroindazolylacetonitriles: efficient synthetic access via vicarious nucleophilic substitution and tautomeric switching mediated by anions, New J Chem, 43 (2019) 14355-67.

[46] F.D. Lowy, Staphylococcus aureus infections, N Engl J Med, (1998) 520-32.

[47] Sadia Afroz, Nobumichi Kobayashi, Shigeo Nagashima, M Mahbub Alam, A B M Bayezid Hossain, M Abdur Rahman, et al., Genetic Characterization of Staphylococcus aureus Isolates Carrying Panton-Valentine Leukocidin Genes in Bangladesh, Jpn J Infect Dis, 61 (2008) 393-6.

[48] L. Drago, E. De Vecchi, L. Nicola, M.R. Gismondo, In vitro evaluation of antibiotics' combinations for empirical therapy of suspected methicillin resistant Staphylococcus aureus severe respiratory infections, BMC Infect Dis, 7 (2007) 1-7.

[49] D.I.V. Andrew Minnock, Jack Schofield, John Griffiths, J. Howard Parish and Stanley B. Brown, Mechanism of Uptake of a Cationic Water-Soluble Pyridinium Zinc Phthalocyanine across the Outer Membrane of Escherichia coli, Antimicrob Agents Chemother, 44 (2000) 522-7.

[50] C. Vieira, A.T.P.C. Gomes, M.Q. Mesquita, N.M.M. Moura, M.G.P.M.S. Neves, M.A.F. Faustino, et al., An Insight Into the Potentiation Effect of Potassium Iodide on aPDT Efficacy, Front Microbiol, 9 (2018).

[51] E.E. Bonfantini, A.K. Burrell, W.M. Campbell, M.J. Crossley, J.J. Gosper, M.M. Harding, et al., Efficient synthesis of free-base 2-formyl-5,10,15,20-tetraarylporphyrins, their reduction and conversion to [(porphyrin-2-yl)methyl]phosphonium salts, J Porphyrins Phthalocyanines, 06 (2002) 708-19.

[52] N.M.M. Moura, M.A.F. Faustino, M.G.P.M.S. Neves, A.C. Duarte, J.A.S. Cavaleiro, Vilsmeier-Haack formylation of Cu(II) and Ni(II) porphyrin complexes under microwaves irradiation, J Porphyrins Phthalocyanines, 15 (2011) 652-8.

[53] T. Hashimoto, Y.-K. Choe, H. Nakano, K. Hirao, Theoretical Study of the Q and B Bands of Free-Base, Magnesium, and Zinc Porphyrins, and Their Derivatives, J Phys Chem A, 103 (1999) 1894-904.

[54] J.S. Baskin, H.-Z. Yu, A.H. Zewail, Ultrafast Dynamics of Porphyrins in the Condensed Phase: I. Free Base Tetraphenylporphyrin, J Phys Chem A, 106 (2002) 9837-44.

[55] J. Durantini, L. Otero, M. Funes, E.N. Durantini, F. Fungo, M. Gervaldo, Electrochemical oxidation-induced polymerization of 5,10,15,20-tetrakis[3-(N-ethylcarbazoyl)]porphyrin. Formation and characterization of a novel electroactive porphyrin thin film, Electrochim Acta, 56 (2011) 4126-34.

[56] A.C. M. Montalti, L. Prodi, M. T. Gandolfi, Handbook of Photochemistry, 3rd ed., Boca Raton: Taylor & Francis; 2006.

[57] P.G. Seybold, M. Gouterman, Porphyrins: XIII: Fluorescence spectra and quantum yields, J Mol Spectrosc, 31 (1969) 1-13.

[58] E.A. Ermilov, S. Tannert, T. Werncke, M.T.M. Choi, D.K.P. Ng, B. Röder, Photoinduced electron and energy transfer in a new porphyrin–phthalocyanine triad, Chem Phys, 328 (2006) 428-37.

[59] A. Gomes, E. Fernandes, J.L.F.C. Lima, Fluorescence probes used for detection of reactive oxygen species, J Biochem Bioph Methods, 65 (2005) 45-80.

[60] E. Zenkevich, E. Sagun, V. Knyukshto, A. Shulga, A. Mironov, O. Efremova, et al., Photophysical and photochemical properties of potential porphyrin and chlorin photosensitizers for PDT, J Photochem Photobiol, B, 33 (1996) 171-80.

[61] M.R. Hamblin, Potentiation of antimicrobial photodynamic inactivation by inorganic salts, Expert Rev Anti Infect Ther, 15 (2017) 1059-69.

[62] L. Huang, A. El-Hussein, W. Xuan, M.R. Hamblin, Potentiation by potassium iodide reveals that the anionic porphyrin TPPS4 is a surprisingly effective photosensitizer for antimicrobial photodynamic inactivation, Photochem Photobiol B, 178 (2018) 277-86.

[63] A.R. Santos, A.F.P. Batista, A.T.P.C. Gomes, M.G.P.M.S. Neves, M.A.F. Faustino, A. Almeida, et al., The Remarkable Effect of Potassium Iodide in Eosin and Rose Bengal Photodynamic Action against Salmonella Typhimurium and Staphylococcus aureus, Antibiotics, 8 (2019) 211.

[64] M.A.F.a.J.P.T. Adelaide Almeida, "Photodynamic inactivation of bacteria: finding the effective targets", Future Med Chem, 10 (2015) 221–1224.

[65] Y. Nitzan, M. Salmon-Divon, E. Shporen, Z. Malik, ALA induced photodynamic effects on Gram positive and negative bacteria, Photochem Photobiol Sci, 3 (2004) 430-5.

[66] G. Bertoloni, F.M. Lauro, G. Cortella, M. Merchat, Photosensitizing activity of hematoporphyrin on Staphylococcus aureus cells, Biochim Biophys Acta, Gen Subj, 1475 (2000) 169-74.

[67] A.A. El-Adly, Photoactive anionic porphyrin derivative against Gram-positive and Gram-negative bacteria, J Appl Sci Res, 4 (2008) 1817-21.

[68] Y. Zhang, T. Dai, M. Wang, D. Vecchio, L.Y. Chiang, M.R. Hamblin, Potentiation of antimicrobial photodynamic inactivation mediated by a cationic fullerene by added iodide: in vitro and in vivo studies, Nanomedicine (Lond), 10 (2015) 603-14.

[69] W. L. F. Armarego, C. Chai, Purification of Laboratory Chemicals, 7th ed. ed., Oxford, UK: Butterworth-Heinemann; 2013.

[70] J.C.J.M.D.S. Menezes, M.A.F. Faustino, K.T. de Oliveira, M.P. Uliana, V.F. Ferreira, S. Hackbarth, et al., Synthesis of New Chlorin e6 Trimethyl and Protoporphyrin IX Dimethyl Ester Derivatives and Their Photophysical and Electrochemical Characterizations, Chem Eur J, 20 (2014) 13644-55.

[71] M.E. Gonçalves, D.; Tomé, R.; Mendes, F.; Valado, A., Armando C., Gabriel, A. and Osório N., Prevalence of the Panton-Valentine Leukocidin in Staphylococcus aureus associated with Upper Respiratory Tract Infections, Int Invention J Med Med Sci, 1 (2013) 8-13.

Highlights

- Synthesis of β-functionalized porphyrin-indazole hybrids *via* Knoevenagel condensation

- Some of the new conjugates showed good capability in the generation of singlet oxygen

- Antimicrobial photodynamic efficiency of the hybrids prepared were evaluated against MRSA bacteria

- The addition of potassium iodide significantly potentiated the aPDT process

Graphical abstract

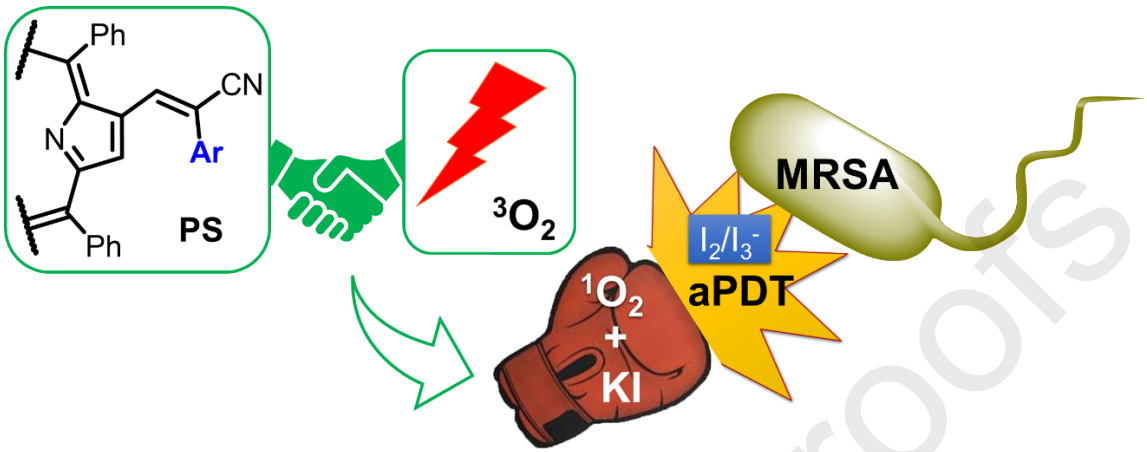

Declaration of interests

☒ The authors declare that they have no known competing financial interests or personal relationships that could have appeared to influence the work reported in this paper.

☐The authors declare the following financial interests/personal relationships which may be considered as potential competing interests: